Direct Observation of Crystal Facet Transformation during Gold-Tin Alloy Electroplating

Zhiwei Chiang

Principal Engineer, Expitaxy Department, Avago Technologies
E-mail: jiangwei68@hotmail.com, Phone: +65 91828611

ABSTRACT

Gold-Tin alloys are commonly used as solder materials in semiconductor industries. In this work, Au-Sn alloys have been electroplated with different bath conditions. For the first time, Au-Sn alloy single crystals have been observed. There are two kinds of single crystals were grown with the compositions of Au_4Sn and Au_2Sn, different from literature-stated Au_5Sn and $AuSn$. The effects of bath composition and plating factors on crsytal facet development of Au-Sn deposits have been investigated. SEM/EDX analysis showed that only Au_4Sn and Au_2Sn phases are single crystals among all plated deposits. The growth of either Au_4Sn or Au_2Sn phases showed preferred orientation with plating conditions. We report on quantitative SEM/EDX characterizations used to study the facet transformation behavior of Au-Sn alloy at the nanometer scale. We have obtained direct evidence that the single crystals and crystal facet transformation of Au_4Sn and Au_2Sn does exist in Au-Sn alloy, and high Sn content enhanced the crystal growth through a spiral-like growth mechanism.

Index Terms: Gold; Tin; Eutectic; Intermetallic compounds; Electroplating;

I. INTRODUCTION

Gold-tin (Au-Sn) eutectic solders are commonly used in the optoelectronic and microelectronic industries for integrated chip or die bonding. Au-Sn solder is becoming the preferred answer to many modern packaging challenges, and widely used as a die attach material for high thermal demand applications, such as microwave devices, laser diodes and RF power amplifiers. Au-Sn is an excellent choice for these applications because of its superior high temperature performance, excellent electrical and thermal conductivity, high mechanical strength, fluxless soldering, and lead-free. One of the drawbacks of Au-Sn is its high cost (80 wt% gold). In addition, Au-Sn can only be used in the situations where the die is able to withstand a temperature above 300 °C for a short duration. Another drawback is that maintaining the desired eutectic composition requires extreme accuracy process control. The phase diagram (Figure 1) shows that the desired 280 °C Au-Sn eutectic point has steep walls. Many researches have been carried out on Au-Sn alloy electroplating and its applications [1-3].

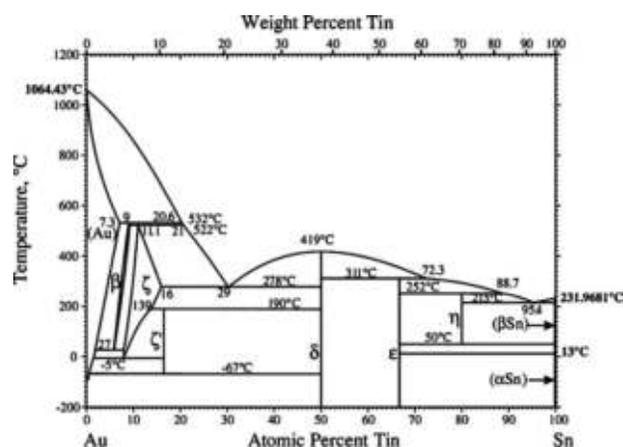During the past few years, new technology has been developed that makes electrolytic plating of

Figure 1. Phase diagram of Au-Sn alloy [4]

Au-Sn material a commercial option. Plating eutectic Au-Sn alloy from a single bath has the potential advantages of achieving the correct composition and preventing Sn oxide formation. Alloy electroplating of Au-Sn eutectic solder is an attractive process due to low cost process, offering the thickness and compositional control, promising better composition control, lower mechanical stress, and finer dimensional capability, with lower processing complexity,

higher throughput, and low capital cost. It offers the economic advantage without oxidation of an outer Sn layer or the formation of unwanted Au-Sn compounds during reflow. The deposited material from solution goes only onto the desired area, as delineated by a photoresist mask, and is therefore more efficient with regard to material consumption. Alloy electroplating of Au-Sn alloys generally involves cyanide-based solutions [4-6], which are desirable from a solution stability standpoint, the deposit composition can be altered by varying the plating conditions [7].

Because of the high stability of Au ions in cyanide complexes, cyanide-based plating baths have been employed by the researchers [8]. Au-Sn alloys were plated out with an acid cyanide system comprising $KAu(CN)_2$, and using pyrophosphate as a complex agent for Sn^{2+} [9]. Au-Sn alloys was also plated out from an alkaline cyanide bath containing $Au(CN)_2^-$, CN^-, SnO_3^{2-}, and PO_4^{3-} [10]. Subsequent research to further improve the bath stability and Au-Sn codeposition has been carried out in the group [11, 12]. The composition of the deposit may be continuously varied during the deposition over the range from 10 to 40 weight-percent Sn by controlling the plating current density. Au_5Sn at low current densities ($<1mA/cm^2$) and AuSn at high current densities ($>2mA/cm^2$) have been separately plated out in the form of intermetallic compounds. These two phases can be combined to produce the eutectic Au-Sn alloy for bonding applications, as well as any alloy with a composition from 15–50 at% Sn. There exist four main Au-Sn intermetallic compounds, Au_5Sn, AuSn, $AuSn_2$, and $AuSn_4$ [10].

Recently, some researchers are focusing on the investigation on the effect of typical morphologies, structures of Au-Sn IMCs (intermetallic compounds) and the associated mechanical properties. The key points are the morphologies of Au-Sn IMCs would affect shear properties of the device packaging remarkably [13-15]. Wang's group studied the orientation relationships and interfaces between ζ'-Au5Sn and metal have been studied by transmission electron microscopy, and discusses the forms of δ-AuSn and ζ'-Au5Sn by heterogeneous nucleation theory [16].

In this work, the different compositions of Au-Sn deposits and intermetallic phases obtained from the plating baths. Bath compositions and plating process parameters were varied in an effort to evaluate the crystal transformation. SEM and EDX spectroscopy were employed to study the Au-Sn compositions and microstructures by varying process parameters which are still stable under experiment conditions and can plate Au-Sn alloys in a reasonably wide operating window.

II. EXPERIMENTAL

Au-Sn alloys were plating from the solution listed in Table 1. The properties of the plated alloys were characterized in the following way: The alloy composition was measured by EDX. The crystal structure and facet transformation were investigated by SEM.

The solution used for electroplating of Au-Sn solders was a weakly acidic, cyanide-based solution, described above, composed of gold and tin salts, as well as a buffering agent and appropriate stabilizers. The cathodes were Si (100) wafers, coated with CVD oxide (5000 nm) and PVD Ti (25 nm)/Au (250 nm) blanket metallization seed layers. Then the wafers were cleaved into 5 cm X 5 cm pieces for plating. Platinum mesh was used as the anode. The electroplating cells were set up with the cathodes facing the anodes spaced 5 cm apart. The temperature of solution was controlled through a hot ultrasonic tank surrounding the electroplating bath, while a thermometer placed inside the electroplating solution monitoring the temperature. The tank transducers produce the high-powered ultrasonic with a frequency of 35 KHz throughout the entire oscillating tank. A secondary bath with same concentrations and temperature, but agitation by a magnetic stirrer, was used to continuously replenish main plating bath at a flow rate of 1.5 litres/minute, same as the pump-out flow rate. Ultrasonic conditions promote the grain size growth, and the replenished bath maintains the solution fresh and concentrated to increase the growth rate too.

Electroplating experiments were carried out with the Sn sulphate varying from 0.1 g/L to 0.3 g/L, and the current density varying from 2 A/dm² to 3 A/dm². This range of solution concentrations and current densities should produce a deposit composition in a wide range for plating done at temperature of 40 °C with ultrasonic agitation. The crystal features and compositions of all the plated materials were examined in a JEOL S-300N scanning electron microscope (SEM), equipped with an EX-220 energy dispersive x-ray (EDX) micro analyzer spectroscopy system. The accelerating voltages of 5 KV and 15 KV were used for imaging and composition analysis, respectively.

Table 1. Acid cyanide based Au-Sn plating solutions used for Au-Sn composition study.

Elements	Concentration
$KAu(CN)_2$	15- 20 g/L
Citric Acid	100-120 g/L
Tin (added as sulphate)	0.1 g/L to 0.3 g/L
pH (adjust with KOH)	3.5-4.5
Temperature	30-50 °C
Current Density	2-3 A/dm²

III.RESULTS AND DISCUSSION

The purpose of the experiments was to study the microstructures by identifying the corresponding facets and their transformations. Facets are indicated by flat regions, possibly containing distinct steps, and bounded by straight edges along regular and reproducible directions.

1. Low Sn Sulphate Concentration Solution

In low Sn sulphate concentration plating solution, at a low current density of 2 A/dm², the main crystal feature produced on the metal coated Si (100) surface was hexagonal crystal with high index forms, as shown in Table 2.

Along with the increasing of current density, the second order prisms of the crystal form {1120} were suppressed. At 2.8 A/dm², the second order prisms of the crystal form {1120} were totally disappeared, polycrystals were observed when current density as high as 3 A/dm², the crystal facet transformation with current densities is shown in Figure 2.

Table 2. Forms present in Au-Sn alloy with hexagonal structure which electroplated from low Sn sulphate solutions with current density of 2 A/dm².
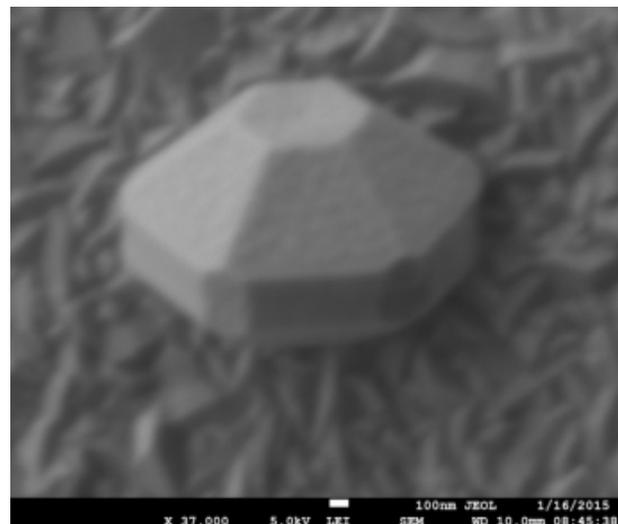
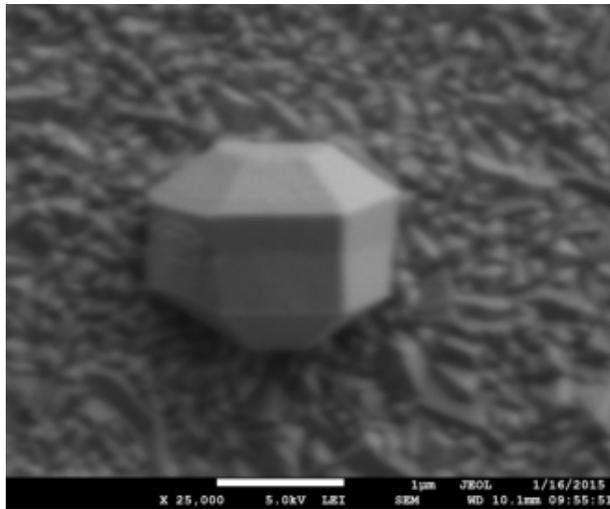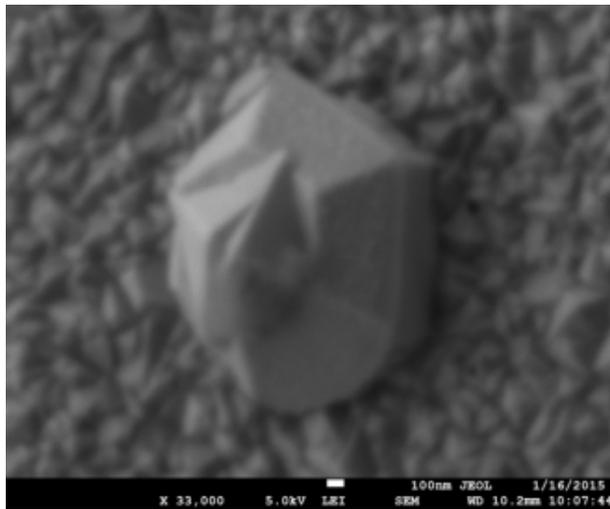| Forms	Number of Faces	Miller Indices
Base	2	{0001}
First order prism	6	{1010}
First order pyramid	12	{1011}
Second order prism	6 (0 at high DK)	{1120}

(B)

(C)

(A)
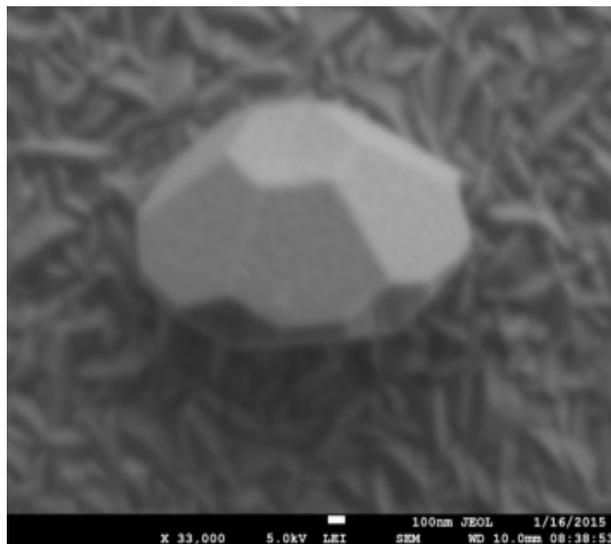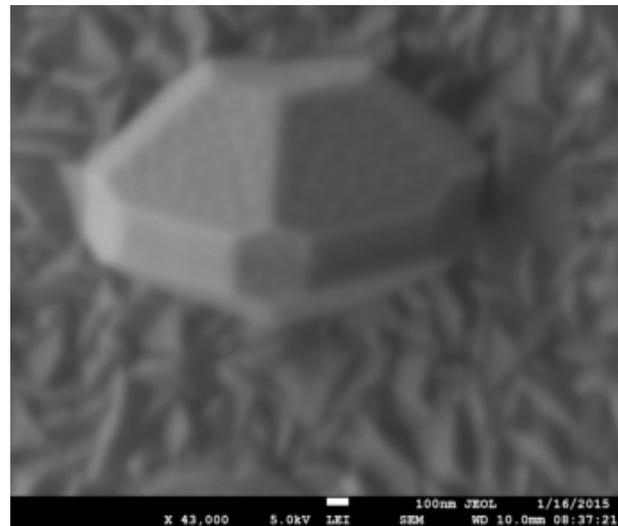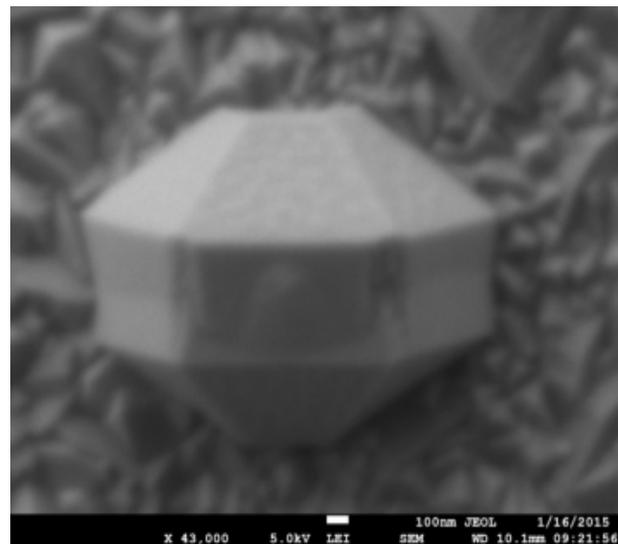
(D)

(E)

(F)

Figure 2. SEM images of Au-Sn alloys electroplated with 0.1 g/L Sn sulphate at current density of: (A) 2 A/dm^2; (B) 2.2 A/dm^2, (C) 2.4 A/dm^2, (D) 2.6 A/dm^2, (E) 2.8 A/dm^2, and (F) 3 A/dm^2.

Furthermore, EDX characterization was carried out on the crystal base (1000) facet, the location and spectrum are shown in Figure 3.

Au-Sn Eutectic compositions are defined as the point on a phase diagram where a two-phase solid freezes from a single-phase liquid. Previous research shows that the two solid phases in the Au-Sn system are both intermetallic compounds, unlike elemental metals in other common eutectics used in electronic applications, such as lead-tin (Pb-Sn) and gold-silicon (Au-Si). In the Au-Si system, the melt at the eutectic composition solidifies to a combination of elemental gold and elemental silicon. For Au-Sn, in contrast, the eutectic melt solidifies into a combination of phase AuSn and phase Au_5Sn. But our work shows the eutectic phase can be a single crystal with a composition of Au_4Sn in hexagonal crystal structure.
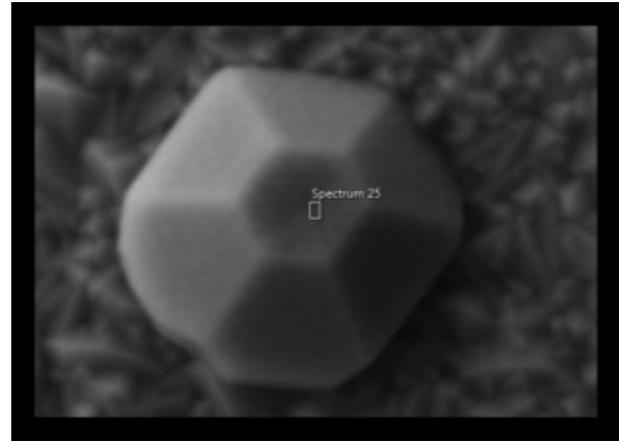
(A)
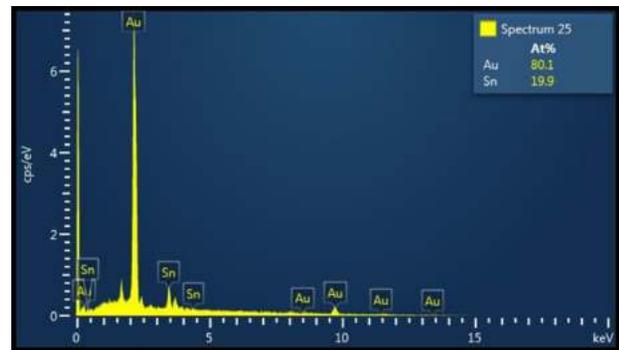
(B)

Figure 3. (A) SEM image of EDX spectrum location on Au_4Sn alloy crystal with well defined crystal forms. (B) EDX spectrum shows the Au-Sn atomic ratio 4:1.

2. High Sn Sulphate Plating Solution

In high Sn sulphate concentration plating solution, at a low current density of 2 A/dm^2, the main crystal feature produced on the metal coated Si (100) surface was a complex edge-transitive (isotoxal) octagon crystal structure with high index forms, as shown in Table 3.

Along with the increasing of current density, the high-index were also suppressed, the trend is similar to what observed on alloy crystals plated from low Sn sulphate concentration solution. The (100) forms were small, with some high-index forms at lower current densities. The high-index forms were disappeared at

Table 3. Forms present in Au-Sn alloy with isotoxal structure which electroplated from high Sn sulphate solutions with current density of 2 A/dm^2.

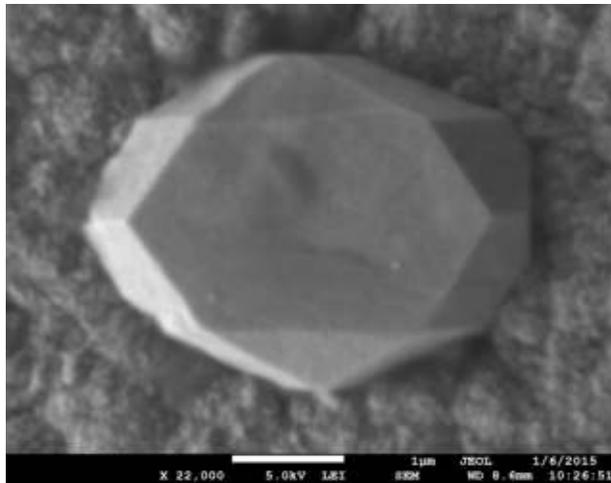| Forms	Number of Faces	Miller Indices
Base	6	{001}
High-index	16	{122}
High-index	4 (0 at high DK)	{310}

2.8 A/dm² with base (100) forms dominantly presented. The polycrystals were also observed when current density as high as 3 A/dm², the crystal facet transformation with current densities is shown in Figure 4.
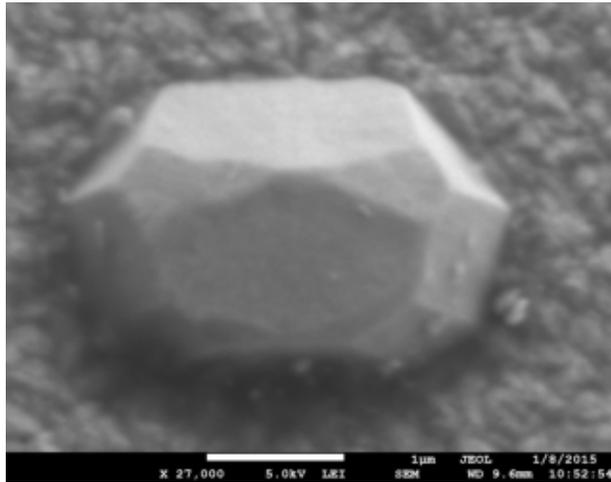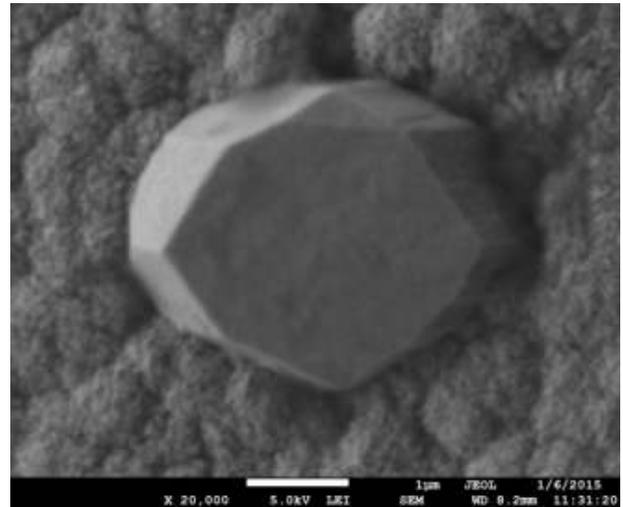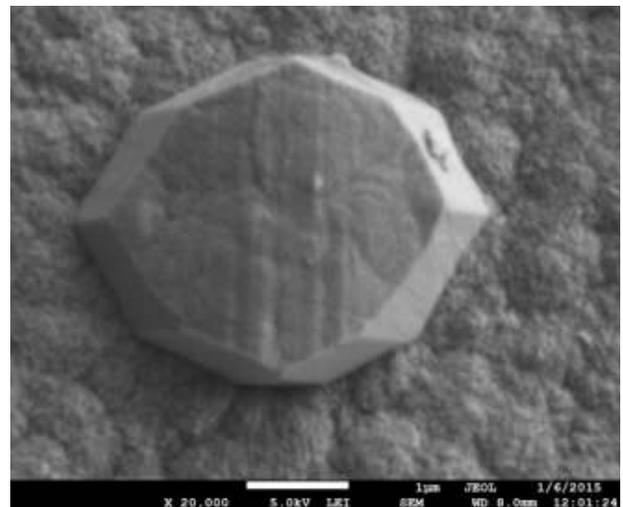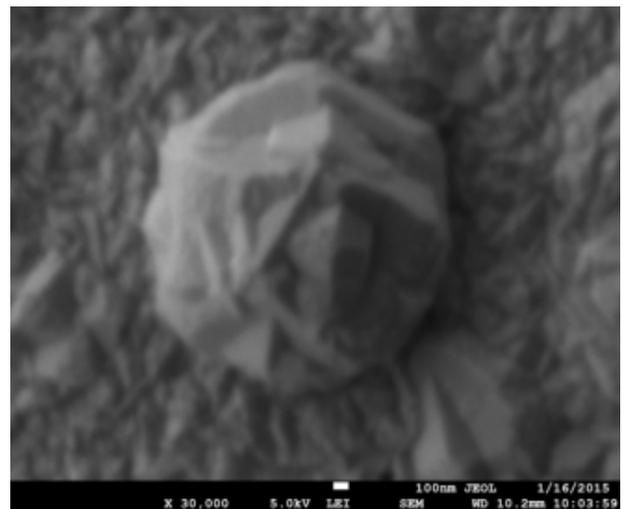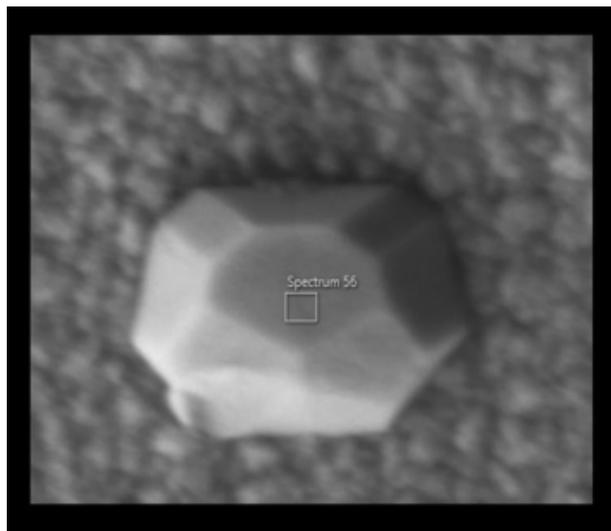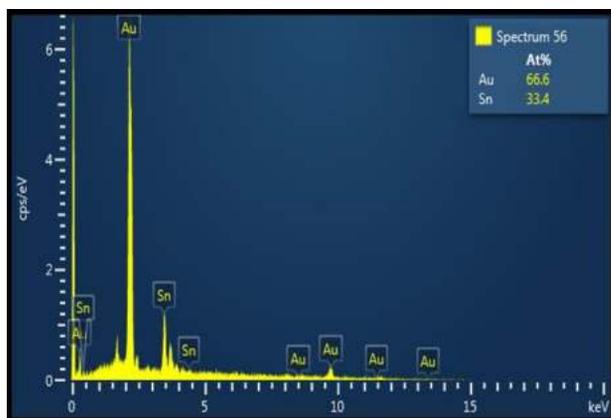

(A)
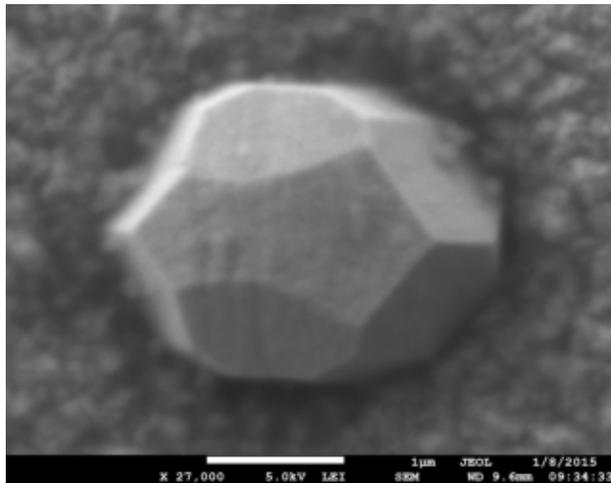
(B)

(C)

(D)

(E)

(F)

Figure 4. SEM images of Au-Sn alloys electroplated with 0.3 g/L Sn sulphate at current density of: (A) 2 A/dm²; (B) 2.2 A/dm², (C) 2.4 A/dm², (D) 2.6 A/dm², (E) 2.8 A/dm², and (F) 3 A/dm².

Growth on a singular surface is constrained by the requirement of nucleation or incorporation of material at particular positions such as kink sites. In Au-Sn cyanide-based acid baths, the degree of faceting can be increased by addition of Sn sulphate to the bath. The faceting is manifested microscopically in the appearance of more facets, more high-index forms and faceted spiral-like growth. Furthermore, EDX characterization was also carried out on the crystal facets, the location and spectrum are shown in Figure 5.

Our work shows that a single crystal with a composition of Au_2Sn in an isotoxal crystal structure is another successful grown Au-Sn alloy crystal. More effects were made to grow other type of single crystals from different concentration solutions, but the outcome was not desired with multi-forms of polycrystals grown, as shown in Figure 6.
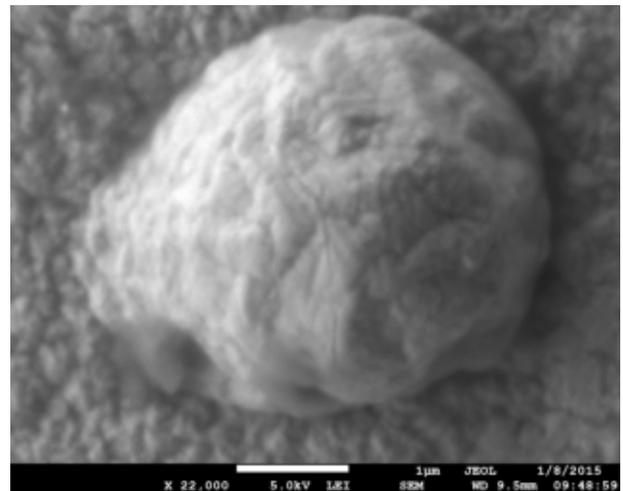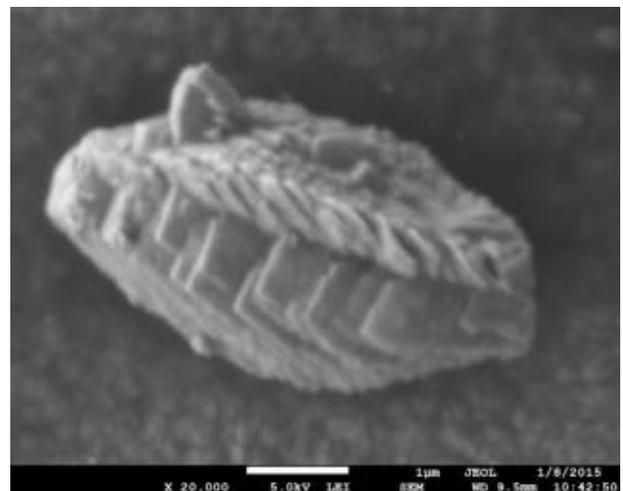

(A)

(B)

Figure 6. SEM images of polycrystal grown from other concentration plating solutions, (A) polycrystal mixed of fine crystal grains, (B) polycrystal with layered crystal grains.

(A)

(B)

Figure 5. (A) SEM image of EDX spectrum location on Au_2Sn alloy crystal with well defined crystal forms. (B) EDX spectrum shows the Au-Sn atomic ratio 2:1.

3. Spiral-like growth on high Sn solution

In a macroscopic description of electroplating, the geometry of the deposit can be fully described by a local velocity given by the current density distribution. The current density in turn depends on bulk-transport and surface kinetic terms. On the microscale, the surface configuration may develop under the control of crystallization steps.

Crystal growth during electroplating has much in common with crystallization from a vapour or a solution. The factor that governs electroplating is the overvoltage that occurs at an electrode during an electrochemical reaction. Depending on the magnitude of the overvoltage, crystal growth may occur by means of spiral-like growth on screw dislocations, the formation

and growth of two-dimensional (2D) crystal nuclei, or the formation of three-dimensional (3D) nuclei. The adsorption of surfactants and the incorporation of impurities have an especially strong effect on the spiral-like growth during electroplating; The formation and growth of 2D nuclei are typical of dislocationless crystals; the formation of 3D nuclei is normally resulting polycrystal if without proper seed crystal and process control. We observed the spiral-like growth mechanism on the isotoxal octagon crystals grown by high Sn sulphate concentration solutions, as shown in Figure 7.

In the case of Au_2Sn growth, spiral-likes are observed on the crystal surface indicating that their growth was driven by screw dislocation mechanism. The spiral-like growth mechanism of Au_2Sn crystals

was enhanced by ultrasonic solution stirring with desired solution replenishing flow rates. At sufficiently high Sn concentration, crystal surfaces do grow from solutions by this mechanism. In contrast, spiral-like growth was not observed on An_4Sn crystals growth at same process condition with lower Sn sulphate concentration. These results indicate that spiral-like hillocks are affected by Sn content transported by a forced solution flow. We concluded that in the case of the spiral-like growth mechanism, a higher Sn concentration is suitable for high quality crystal growth with a faster growth rate. But at low Sn concentration, spiral-like hillocks were suppressed. Based on the theory of spiral-like growth, Sn sulphate acted as impurity clusters and defect centres during Au_2Sn growth, which caused the screw dislocation formation and spiral-like growth initialization.

From our work, Sn in Au-Sn did not change with increasing current density. This trend is agreed that alloy composition is mainly sensitive to the Au ion concentration in the bath. It can also be observed that the Sn content is increased with increasing Sn sulphate, but the incorporation ratio is not linear. Since more Sn in solution than needed, the excess Sn ions may form big molecule clusters which attached on alloy surface as defect centre to initialize and promote spiral-like growth in high Sn sulphate solution.

IV. CONCLUSION

Au_4Sn and Au_2Sn alloy single crystals have been first-time ever observed and confirmed, which are disagreed with literature-stated Au_5Sn and AuSn forming eutectic alloy. The plated Au_4Sn and Au_2Sn alloy single crystals have singular surfaces and exhibit terraces with well-defined crystal orientation and edges.

Au-Sn alloy plated from a weakly acidic, cyanide-based solution, composed of gold and tin salts, buffering agent and appropriate stabilizers may undergo current density-induced faceting transitions at our process conditions. The degree of faceting increases with decreasing current density or increasing Sn sulphate content in cyanide-based solution. Faceting is promoted by Sn sulphate when it is present at high concentration, even acting as a defect centre for spiral-like growth. The high index forms in Au-Sn alloys evidently can be suppressed by high current density. During deposition, these high index forms disappear or replaced by base forms along close-packed directions. It is proposed that the formation of an ordered Au-Sn overlayer on the PVD metal surface, and the resulting in single crystal growth, accounts for the singular growths.
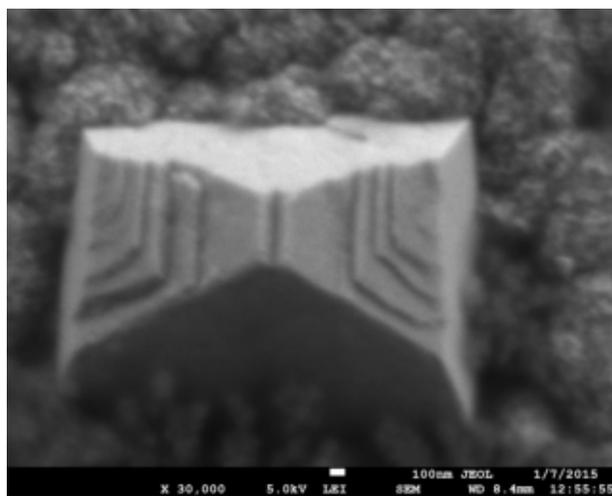
(A)
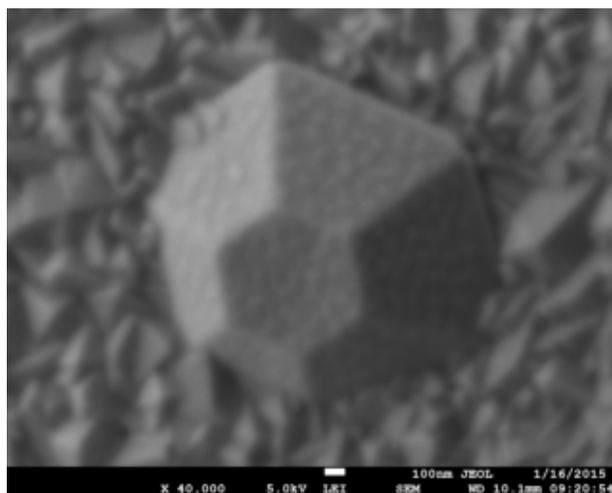
(B)

Figure 7. SEM images of (A) spiral-like growth on isotoxal octagon crystal and (B) non spiral-like growth on hexagonal crystal, plated from different Sn sulphate concentration solutions.

ACKNOWLEDGEMENTS

REFERENCES

[1] Robert S. Forman & Gerard Minogue, Chip Scale Review 8, 55 (2004).

[2] A. He, Q. Liu and D. G. Ivey, J. Mater. Sci. - Mater. Electron. 17, 63 (2006).

[3] W. Sun and D. G. Ivey, Materials Science and Engineering, 65B, 111 (1999).

[4] J. Ciulik & M. R. Notis, Journal of Alloys and Compounds 191, 71 (1993).

[5] G. Holbrom, J.A. Abys, H.K. Straschil, M. Svensson, Plating and Surface Finishing 85, 66 (1998).

[6] N. Kubota, T. Horikoshi and E. Sato, J Met. Fin. Soc. Japan 34, 37 (1983).

[7] B. Djurfors and D.G. Ivey, Materials Science and Engineering B 90, 309 (2002).

[8] G. G. Stanley, The Extractive Metallurgy of Gold in South Africa, edited by The South African Institute of Mining and Metallurgy, Vol. 2, (1987), chap. 15, p.842.

[9] N. Kubota, T. Horikoshi and E. Sato, J Met. Fin. Soc. Japan 34, 37 (1983).

[10] G. Holmbom, J. A. Abys, H. K. Straschil and M. Svensson, Plating & Surface Finishing 85, 66 (1998).

[11] B. Djurfors and D. Ivey, in: GaAs Mantech Conference, Las Vegas, USA, 2001, (May 2001), pp. 196-199.

[12] A. He, B. Djurfors, S. Akhlaghi and D. G. Ivey, in: AESF SUR/FIN 2002 Proceedings, Chicago, USA, 2002, (June 2002), pp. 204-216.

[13] Yali Tian, Zhou Wei, Wu Ping, Journal of Electronic Materials, 2015, 1.

[14] Wei Liu, Rong An, Chunqing Wang, Yanhong Tian, Soldering & Surface Mount Technology, 27 (1), 45 (2015).

[15] Volodymyr Bushlya, Masoomeh Ghasemi, Sven Lidin, Martin Valldor, Fei Wang, Journal of Materials Science, 50 (23), 7808 (2015).

[16] Kuang-Kuo Wang, Bo-Han Jiang, Dershin Gan, Thin Solid Films, 589, 584 (2015).